Journal of Electronic Materials (2021) 50:4850–4857
https://doi.org/10.1007/s11664-021-09033-0

ORIGINAL RESEARCH ARTICLE

# Theoretical and Experimental Study of Optical Response of Bimetallic Platinum and Gold Nanoparticles: Nanoalloys and Core/Shell Configurations

**O. Rocha-Rocha[1,2] · M. Cortez-Valadez[3] · R. García-Llamas[1] · G. Calderón-Ayala[1,4] · P. G. Maní-González[5] · M. Flores-Acosta[1]**

Received: 15 December 2020 / Accepted: 20 May 2021 / Published online: 3 June 2021


## Abstract

In this research, a theoretical and experimental study of bimetallic gold and platinum nanoparticles is reported. From the green synthesis approach, a combination of rongalite with sucrose is used as a reducing and stabilizing agent. Nanoalloys (Au@Pt) and Pt-core/Au-shell nanoparticles were obtained according to the synthesis process used, and the optical response was analyzed. For nanoalloys, two absorption bands were associated with localized surface plasmon resonances. These were located at 300 nm and another between 350 nm and 365 nm, respectively. For core/shell type nanoparticles, an absorption band centered at 530 nm was observed. The images obtained by transmission electronic microscopy (TEM) confirmed the presence of quasi-spherical nanoparticles with core/shell type configurations. Numerical calculations of the cross sections for a Pt-core/Au-shell nanoparticle with spherical geometry was used to establish a comparison with the experimental absorption in the ultraviolet-visible (UV–Vis) spectrum. Complementary, the TEM images and chemical analysis by energy dispersive spectroscopy (EDS) showed the presence of core/shell type nanoparticles.

**Keywords** Bimetallic nanoparticles of au@pt · nanoalloys · core/shell nanoparticles · cross sections

## Introduction

The study of bimetallic nanoparticles (NPs) has become relevant within the interest of researchers since they present new optical properties[1, 2] and can be used in catalysis[3–5], among others, compared to monometallic particles. This has been achieved through the generalization of Mie's theory extended to a core/shell nanoparticle (NP) developed by Aden and Kerker[5]. In this sense, several works have focused on understanding the interaction of electromagnetic waves with core/shell systems as spherical symmetry. Nomura and Takaku [6] have studied the propagation of electromagnetic waves in an inhomogeneous medium by using the rigorous solution of Maxwell's equations. This led to the description of electromagnetic waves propagation across the atmosphere (it was treated like many concentric spheres). This same model was applied to water drops in a cloud, with core/shell configurations on carbon particles as the core of the drop. The generalization of the scattering effects and electromagnetic plane wave by a core/shell NP with spherical symmetry was performed by Wait for any number of concentric regions[7]. One of the first studies with computational support

✉ O. Rocha-Rocha
osnaider.1007@gmail.com

1 Departamento de Investigación en Física, Universidad de Sonora, Apdo. Postal 5-88, 83190 Hermosillo, Sonora, México

2 Grupo de Espectroscopía Óptica y Láser, Departamento de Física, Universidad Popular del Cesar, Apdo Postal 200001, Sabanas Diagonal 21 No. 29-56 Sabanas del Valle, Valledupar, Cesar, Colombia

3 CONACYT - Departamento de Investigación en Física, Universidad de Sonora, Apdo. Postal 5-88, 83190 Hermosillo, Sonora, México

4 Universidad Estatal de Sonora, Rosales No. 189 Col. Centro, 83100 Hermosillo, México

5 Departamento de Física y Matemáticas, Instituto de Ingeniería y Tecnología, Universidad Autónoma de Ciudad Juárez, Ave. Del Charro 450, 32310 Cd. Juárez, Chihuahua, México

for the optical properties of core/shell particles was carried out by Fenn and Oser[8]. In this sense, several investigations have been developed, e.g., Fen[8] found that when the radius of a core is small compared to the outer radius of the NP, the optical properties are almost entirely determined by the excitation of localized surface plasmon resonances (LSPR) on the shell surface. Espenscheid et al.[9] showed that the structure of such nanoparticles can be determined by analysis of electromagnetic radiation scattering data. Kattawar[10] has applied Mie's theory to study the electromagnetic scattering of coated poly-disperse spheres, by considering dry and wet aerosols, as well as water-coated spheroidal core. Gold and silver core/shell configurations have been the most studied, as well as either of these metals combined with a dielectric core. Several works focus on the properties of bimetallic nanoparticles of Au-core/Pt-shell, e.g., their optical resonance[11]. Experimental works have focused on designing core/shell configurations with the purpose of studying optical, electrochemical, and other properties compared to monometallic systems. However, to design perfect core/shell configurations remains a challenge today. Lapp et al.[12] with an electrochemical approach tried unsuccessfully to deposit platinum monolayers on a gold core to study their structural properties. Nevertheless, they obtained NPs smaller than 2 nm of diameter with an optical response in the UV-Vis absorption spectrum presenting two bands with maxima around to 220 nm and 500 nm. These are associated with LSPR for platinum and gold, respectively. The study developed by Yang et al.[13] reported that the order in which the NPs are synthesized influences in the formation of the nanostructures leading in some cases to a simple physical mixture of the elements. Zhang et al.[14] showed that Au-core/Pt-shell nanoparticles have a high catalytic activity compared to platinum NPs. They attributed this to gold core electrons attracting platinum electrons, causing a deficiency of electrons in the shell to promote substrate adsorption with the polar carboxyl groups. In previous research, we reported the synthesis of Au@Cu nanoparticles under ambient conditions by using the combination of rongalite and sucrose as reducing and stabilizing agents, respectively[15].

In this work, we report the synthesis of Au@Pt nanoalloys and Pt-core/Au-shell type structures. Additionally, by using the generalized Mie's theory we present numerical calculations of the extinction and scattering cross sections separately of a Pt-core/Au-shell NP, gold sphere, platinum sphere embedded in a dielectric medium with refractive index equal to water ($n = 1.33$). Furthermore, a comparison study between the UV–Vis absorption spectrum of the Pt-core/Au-shell NPs and the cross sections calculate with the generalized Mie's theory, was carried out.

However, experimental designs involving environmentally friendly methods to obtain stable bimetallic configurations remain a huge challenge today. Therefore, the research aims to provide an effective method for nanoparticle synthesis that allows the study and correlation of the optical properties of absorption.

## Materials and Methods

The ion precursors $Au^{3+}$ and $Pt^{4+}$ were obtained from $[HAuCl_4 \cdot 3H_2O]$ and $[H_2PtCl_6 \cdot (H_2O)_6]$ salts, respectively (*Sigma-Aldrich Co.*). All precursors were prepared with a molarity of 0.01 M in an aqueous solution. Two different methodologies were used. For the first case, we consider the methodology reported in previous work[15] to obtain Au@Pt nanoalloys. Additionally, to obtain Pt-core/Au-shell, the precursors of $Pt^{4+}$ ions were grown during 18 h to conform the platinum-core; subsequently, the precursors of $Au^{3+}$ ions and 0.1 ml of formula T[15] solution was added to obtain gold-shell. In this case, the volume ratios of precursors of ions $Pt^{4+}$ and $Au^{3+}$ were 5:1, respectively (see Fig. 1 bottom). In the Fig. 1 we show the synthesis process used in this paper to obtain the nanoparticles.

## Numerical Details

The level theory used in this work to study the diffraction of an incident monochromatic electromagnetic plane wave with a core/shell nanoparticle with spherical symmetry was reported by Aden and Kerker[5], which correspond to an extension of Mie's theory.

We developed a computer code for the calculations of the optical properties based on the generalized Mie's theory. It was necessary because we calculate the near electric field generate by the core/shell nanoparticle and the spectral response for absorbing material. This is not found on the BHCOATED[16] (these results are not shown in this paper).

The electromagnetic fields are expressed in their multipolar expansion as follows[17, 18]:

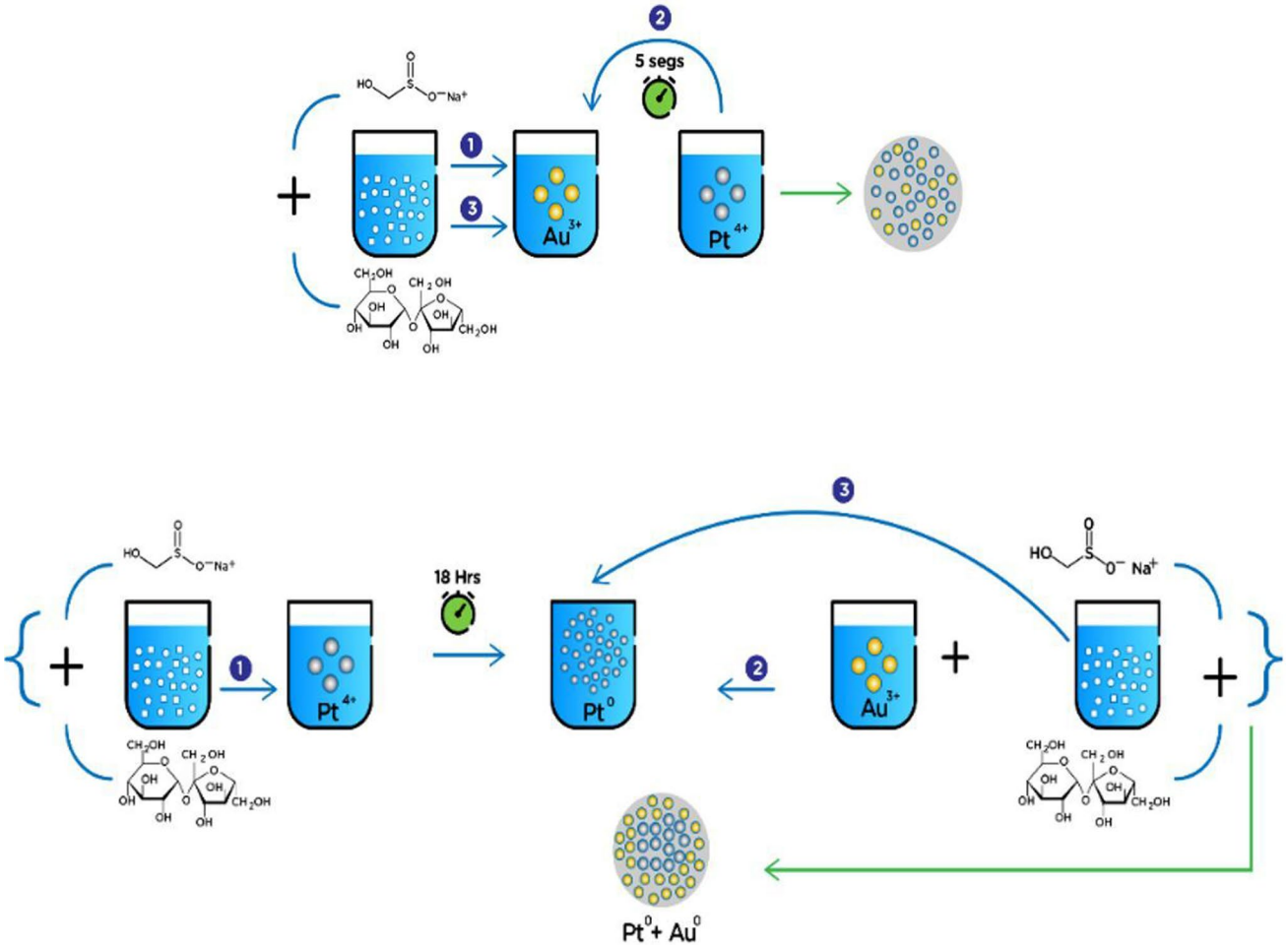


**Fig. 1** Schematic representation of the experimental methodology used to obtain, top: nanoalloys, and bottom: core/shell nanoparticles.

$$\vec{E}^{(m)}(\vec{r}) = Z_m \sum_{l=1}^{\infty} \left\{ \begin{array}{l} a_{l,1}^{(m+)} f_l(q_m r)\left[\vec{X}_{l,1}(\theta,\varphi) - \vec{X}_{l,-1}(\theta,\varphi)\right] + \dfrac{ib_{l,1}^{(m+)}}{q_m r}\dfrac{\mathrm{d}}{\mathrm{d}r}\left[r f_l(q_m r)\right]\hat{r} \\ \times\left[\vec{X}_{l,1}(\theta,\varphi) + \vec{X}_{l,-1}(\theta,\varphi)\right] - \dfrac{b_{l,1}^{(m+)}}{q_m}\sqrt{l(l+1)}\left[Y_{l,1}(\theta,\varphi) + Y_{l,-1}(\theta,\varphi)\right]\dfrac{f_l(q_m r)}{r}\hat{r} \end{array} \right\} + \left\{ \begin{array}{l} a_{l,1}^{(m-)} g_l(q_m r)\left[\vec{X}_{l,1}(\theta,\varphi) - \vec{X}_{l,-1}(\theta,\varphi)\right] + \dfrac{ib_{l,1}^{(m-)}}{q_m r}\dfrac{\mathrm{d}}{\mathrm{d}r}\left[r g_l(q_m r)\right]\hat{r} \\ \times\left[\vec{X}_{l,1}(\theta,\varphi) + \vec{X}_{l,-1}(\theta,\varphi)\right] - \dfrac{b_{l,1}^{(m-)}}{q_m}\sqrt{l(l+1)}\left[Y_{l,1}(\theta,\varphi) + Y_{l,-1}(\theta,\varphi)\right]\dfrac{g_l(q_m r)}{r}\hat{r} \end{array} \right\} \tag{1}$$

$$\vec{H}^{(m)}(\vec{r}) = \sum_{i=1}^{\infty} \left\{ \begin{array}{l} b_{l,1}^{(m+)} f_l(q_m r)\left[\vec{X}_{l,1}(\theta,\varphi) + \vec{X}_{l,-1}(\theta,\varphi)\right] - \dfrac{i a_{l,1}^{(m+)}}{q_m r}\dfrac{\mathrm{d}}{\mathrm{d}r}\left[r f_l(q_m r)\right]\hat{r} \\ \times\left[\vec{X}_{l,1}(\theta,\varphi) - \vec{X}_{l,-1}(\theta,\varphi)\right] + \dfrac{a_{l,1}^{(m+)}}{q_m}\sqrt{l(l+1)}\left[Y_{l,1}(\theta,\varphi) - Y_{l,-1}(\theta,\varphi)\right]\dfrac{f_l(q_m r)}{r}\hat{r} \end{array} \right\} + \left\{ \begin{array}{l} b_{l,1}^{(m-)} g_l(q_m r)\left[\vec{X}_{l,1}(\theta,\varphi) + \vec{X}_{l,-1}(\theta,\varphi)\right] - \dfrac{i a_{l,1}^{(m-)}}{q_m r}\dfrac{\mathrm{d}}{\mathrm{d}r}\left[r g_l(q_m r)\right]\hat{r} \\ \times\left[\vec{X}_{l,1}(\theta,\varphi) - \vec{X}_{l,-1}(\theta,\varphi)\right] + \dfrac{a_{l,1}^{(m-)}}{q_m}\sqrt{l(l+1)}\left[Y_{l,1}(\theta,\varphi) - Y_{l,-1}(\theta,\varphi)\right]\dfrac{g_l(q_m r)}{r}\hat{r} \end{array} \right\} \tag{2}$$

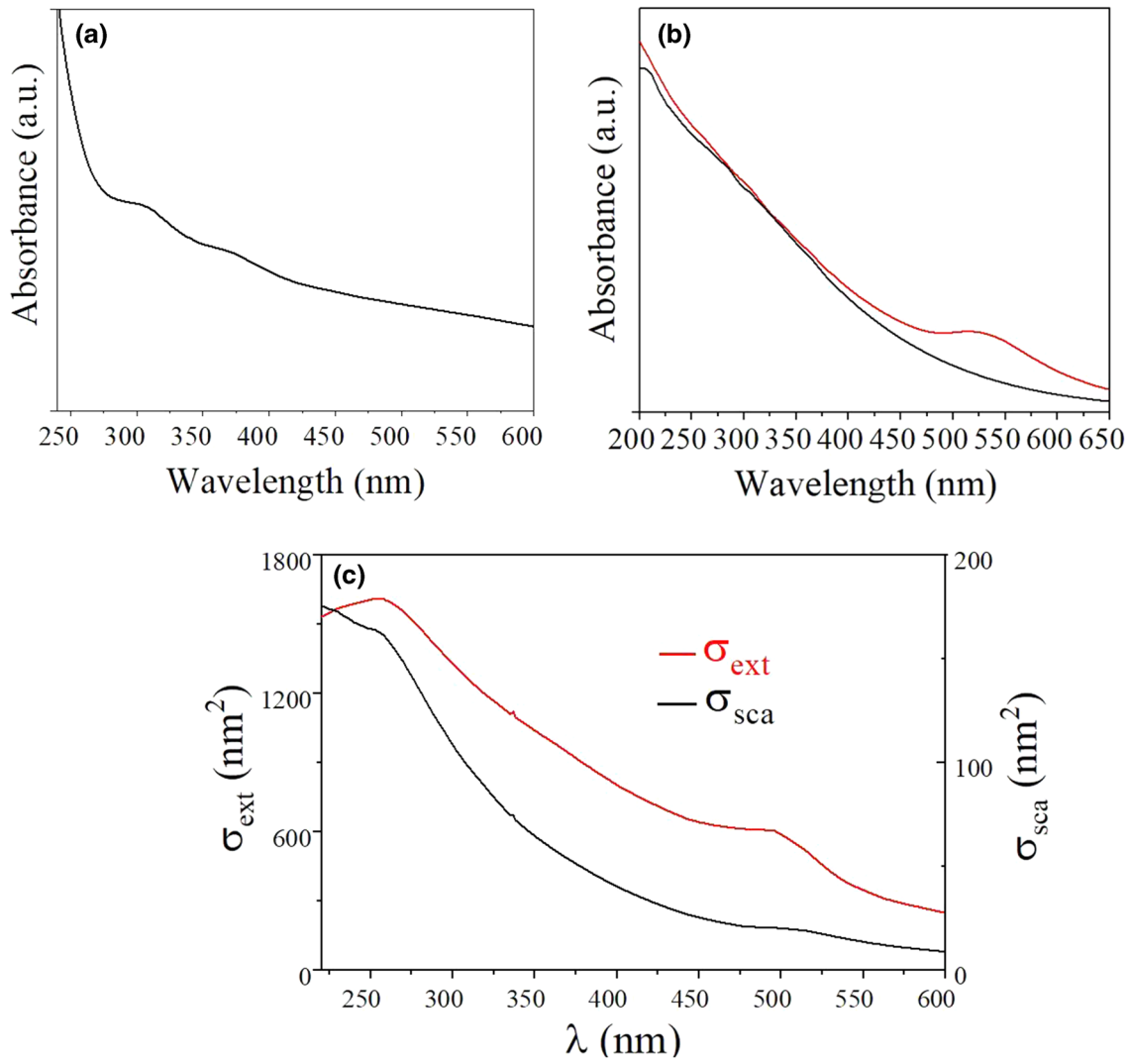


**Fig. 2** UV-Vis absorption spectrum of (a) Au@Pt NPs nanoalloys, (b) Pt NPs (black line) and Pt@Au nanoparticles (red line). (c) Extinction (red line) and scattering cross section (black line) of a Pt-core/Au-shell nanoparticle embedded in water (1.33) with internal and external radii of 14 and 16 nm, respectively. The extinction ($\sigma_{ext}$) and scattering cross section ($\sigma_{sca}$) were calculated with Eqs. 3 and 4 (Color figure online).

where $m = 1, 2, 3$ indicates the core, shell and embedded medium, respectively. $q_m$ is the wavenumber of the medium,$Y_{l,\pm1}(\theta, \varphi)$ and $\vec{X}_{l,\pm1}(\theta, \varphi)$ are the scalar and vector spherical harmonics, respectively. $Z_m$ is the impedance of the medium. $f_l(q_m r)$ and $g_l(q_m r)$ are the spherical Bessel functions. In the core $f_l(q_m r) = j_l(q_1 r); a_{l,1}^{(1-)} = b_{l,1}^{(1-)} = 0$. In the shell $f_l(q_m r) = j_l(q_2 r); g_l(q_m r) = n_l(q_2 r)$ and for the embedded medium $f_l(q_m r) = j_l(q_3 r)$; $g_l(q_m r) = h_l^{(1)}(q_3 r)$.

The extinction ($\sigma_{ext}$) and scattering ($\sigma_{sca}$) cross sections of a spherical core/shell nanoparticle with inner and outer radii $R_1$ and $R_2$, respectively, at a wavelength $\lambda$ in vacuum, can be expressed by an infinite series, as follows [16]:

$$\sigma_{ext} = \frac{2\pi}{q_3^2} \sum_{l=1}^{\infty} (2l+1) \mathrm{Re}\left(a_{l,1}^{(s)} + b_{l,1}^{(s)}\right) \tag{3}$$

$$\sigma_{sca} = \frac{2\pi}{q_3^2} \sum_{l=1}^{\infty} (2l+1) \mathrm{Re}\left(\left|a_{l,1}^{(s)}\right|^2 + \left|b_{l,1}^{(s)}\right|^2\right) \tag{4}$$

where $q_3 = 2\pi n_3/\lambda$ is the magnitude of the wave vector and $n_3$ is the refractive index of the external medium (water in this case, $n_3 = 1.33$). The scattered coefficients $a_{l,1}^{(s)}$ and $b_{l,1}^{(s)}$ are determined by boundary conditions of the electromagnetic fields on the inner and outer shell surfaces. These represent the amplitudes of oscillations of magnetic and electric multipole type, respectively. To establish the convergence pattern for $\sigma_{ext}$ and $\sigma_{sca}$ we fixed the $\lambda$ (position of LSPR) and the cross sections were calculated as a function of $l$. In this study, we have considered $l = 1$ because we assume that variations under 1% are sufficient to establish convergence in $\sigma_{ext}$ and $\sigma_{sca}$.

We consider a Pt-core/Au-shell nanoparticle embedded in a dielectric medium with refractive index $n = 1.33$, i.e., water. The inner and outer radii of the Pt-core/Au-shell nanoparticle were fixed to 14 and 16 nm, respectively. Furthermore, the cross sections for a gold and platinum sphere with radius of 16 nm, were calculated. The values of dielectric functions for gold and platinum correspond to the bulk metals [19].

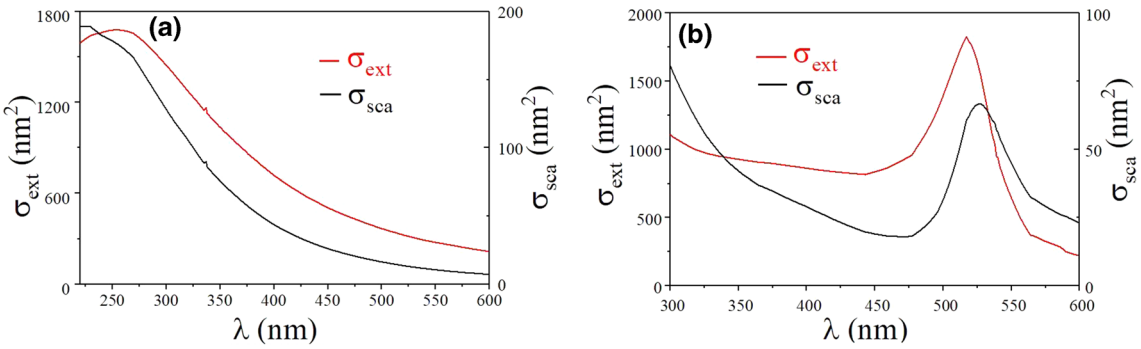


**Fig. 3** Extinction (red line) and scattering cross section (black line) of a (a) platinum sphere and (b) gold sphere. The radii of the spheres are 16 nm, and the embedded medium is water ($n = 1.33$). The extinction ($\sigma_{ext}$) and scattering cross section ($\sigma_{sca}$) were calculated with Eqs. 3 and 4 (Color figure online).

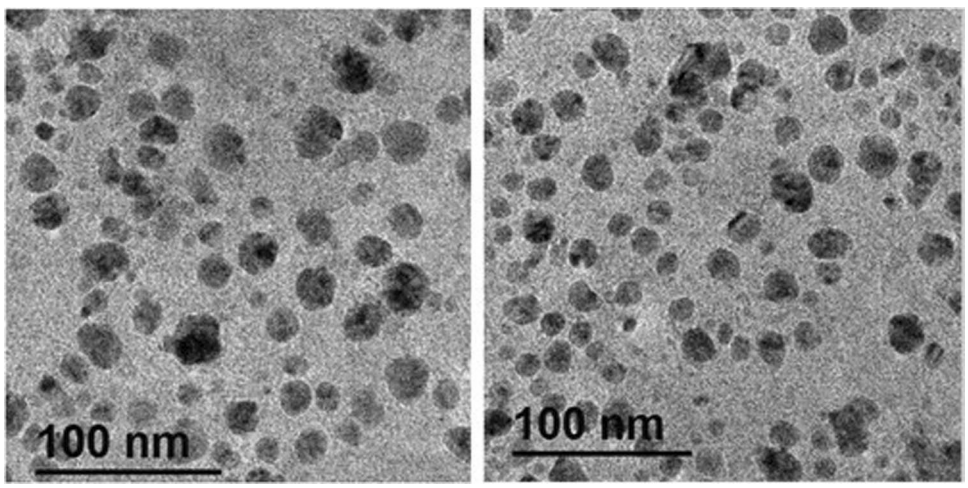


**Fig. 4** TEM images of Pt@Au NPs (both images correspond to the sample with the UV–Vis spectrum in the Fig. 2b, red line) (Color figure online).

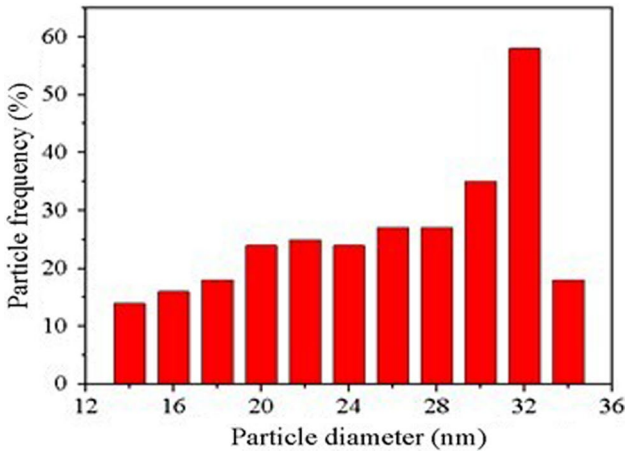


**Fig. 5** Particle size histogram obtained from Fig. 4.

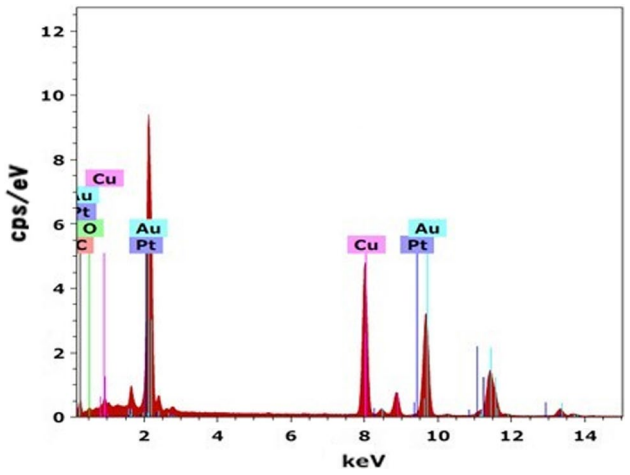


**Fig. 6** Chemical composition by EDS of Pt@Au NPs (from TEM image in Fig. 4)

## Results and Discussion

Figure 2a shows the UV–Vis optical absorption spectrum of Au@Pt nanoalloys. Two maximum signals are observed and correspond to the excitation of LSPR; the first one is located around 300 nm and the other between 350 and 365 nm. These two optical responses are related to the atomic composition/distribution of the gold and platinum atoms on the surface of the nanoparticles, i.e., the optical response can be described as LSPR "hybrid" due to the contributions of the interference of LSPR associated with gold and platinum metals. This may be associated with a theoretical approach, as the response associated with the selection of a dielectric function determined by the contribution of the dielectric functions of the metals. The simplest method is a simple linear combination of the dielectric functions of individual metals, which is considered the standard method for alloys[20]. When in the synthesis process, the core (platinum) is grown for 18 h, and later the second metal to conform the shell (gold) is added, the optical response is different. The Fig. 2b (red line) shows the UV–Vis absorption spectrum of Pt-core/Au-shell nanoparticles, the position at 530 nm is associated with LSPR of nanoparticles with gold-rich surfaces including a damping on its intensity due to the presence of a second metal, i.e., platinum[21]. The Fig. 3b shows the extinction ($\sigma_{ext}$) and the scattering ($\sigma_{sca}$) of a gold sphere with a radius of 16 nm calculated with generalized Mie's theory, Eqs. 3 and 4, respectively. The relative maximum in Fig. 3 correspond to the LSPR. The LSPR position in the $\sigma_{ext}$ located at 517 nm and at 527 nm in the $\sigma_{sca}$, agree with experimental works on gold nanoparticles, e.g., as some results reported previously[11, 15]. The difference in the UV–Vis absorption spectrum profile of the Pt-core/Au-shell nanoparticles with respect to the AuNPs[11, 15] and the cross sections of the gold sphere in Fig. 3b is associated with the presence of the platinum core. This behavior (Fig. 2b, red line) suggests that the contribution of the dissipation energy due to the platinum's core is responsible for the damping of the absorption spectrum[21] in Fig. 2b (red line). For Pt NPs, the maximum in the absorption band appears in the UV region of the electromagnetic spectrum around 215–220 nm (Fig. 2b, black line), which is characteristic of the LSPR of these nanoparticles[21]. The UV–Vis absorption spectrum profile of Pt NPs in the Fig. 2b (black line) is in agreement with the $\sigma_{ext}$ and the $\sigma_{sca}$ spectrum profile of a platinum sphere of radius of 16 nm calculated using Mie's theory in Fig. 3a. The intensity of the absorption decreases (see Figs. 2 and 3a) with the increase of the wavelength since the Pt NPs have the position of the LSPR in the ultraviolet region, unlike metals as Ag and Au whose LSPR are in the region of the visible one. This characteristic is attributed to the interband excitations with the excitation of the LSPR in Pt NPs that take place in the UV region.

The difference between LSPR position (in the region of 215–220 nm) for Pt NPs (Fig. 2b, black line) with respect to the cross sections, 250 nm in the $\sigma_{ext}$ and 230 nm in $\sigma_{sca}$ (Fig. 3a) is related to the higher particle size distribution as shown in Fig. 5 and different geometries of Pt NPs in Fig. 4.

The Fig. 2c shows the spectrum of $\sigma_{ext}$ and $\sigma_{sca}$ of a Pt-core/Au-shell nanoparticle obtained from Eqs. (3) and (4), respectively. All calculations of $\sigma_{ext}$ and $\sigma_{sca}$ correspond to the dipolar contribution in Eqs. (3) and (4), i.e., $l$=1.

The theoretical spectrum profile is very similar to the UV–Vis absorption spectrum of the nanoparticles obtained experimentally. (Fig. 2b, red line). This may suggest that the optical response of the NPS is due to the presence of gold on the surfaces of the nanoparticles and the last ones can be roughly considered as core/shell configurations.

The Fig. 6 shows the chemical analysis of Pt-core/Au-shell nanoparticles by EDS. This Figure shows higher contents of Au and Pt, which suggest that the NPs with optical response in the Fig. 2b (red line) correspond to the combination of Pt and Au. This is consistent with the synthesis process (Fig. 1). The difference between the bandwidth and the LSPR position (Fig. 2b, red line) with respect to the theoretical calculation (Fig. 2c) is attributed to several reasons. e.g., the presence of a high particle size distribution (Fig. 5) [22], several geometries[23], among other characteristics of NPs: inhomogeneous thicknesses and, the fact that not all NPs are perfectly spherical, as TEM image shows in the Fig. 4. In addition, as shown in Fig. 4, the cores are not perfectly spherical and not concentric with respect to the shell. This explains the differences in the position of LSPR, which in the case of extinction and scattering cross sections are located at lower wavelengths with respect to the UV-Vis absorption spectrum (Fig. 2b, red line). It is well known that the dispersive dielectric function of metal depends on the particle's size. For example, particles with diameters larger than 10 nm, their dielectric functions are size independent[24], while for particles with a diameter smaller than 10 nm, their dielectric functions are size dependent, i.e., LSPR as a function of particle radius must be considered[25]. Figure 5 shows that nanoparticle's diameter varied between 14 and 34 nm. Figure 4 shows particles with different geometries and spaced at a distance smaller than their diameters. This causes the scattered partial waves to interfere (see Fig. 2.72 in [24]) and is possibly the main reason for the redshift of LSPR of the nanostructures in comparison with the cross sections. However, the extinction and scattering cross section spectra for a Pt-core/Au-shell with inner and external radii of 14 nm and 16 nm, respectively (shown in Fig. 2c) are in good agreement with the UV-Vis spectrum for Pt@Au nanoparticles as shown in Fig. 2b (red line). Furthermore, the presence of gold and platinum is confirmed for the chemical composition by EDS study, as is shown in Fig. 6. This suggests that the Pt@Au nanoparticles can be considered Pt-core/Au-shell nanoparticles or core/shell approximations. The agreement between the experimental and theoretical results for the case of the LSPR position, especially for the case of the scattering cross section, is associated with the fact that the surfaces of the nanoparticles are rich in gold. Furthermore, the dispersion of electromagnetic waves by NPs is more significant compared to the absorption. However, the LSPR position is closer to the maximum in the scattering cross-section (Fig. 2c, black line) compared to the extinction cross section tending to shift to lower wavelengths, as shown in Fig. 2c (red line).

## Conclusions

Through the synthesis process used in this work, bimetallic Au@Pt nanoparticles were obtained. First, when metals are combined simultaneously, alloy nanostructures are obtained. Second, when the platinum core is grown for 18 h and then second metal (gold) is added, nanostructures that tend to core/shell configurations are obtained. A significant difference between the two synthesized systems is evident in their UV-Vis absorption spectra. The positions of the maxima in the absorption band for the LSPR of the Au@Pt nanoalloys are around 300 nm and another between 350 nm and 365 nm. For Pt-core/Au-shell configurations, there is a maximum in 530 nm corresponding to the NPs with gold-rich surfaces. The calculation of the extinction and scattering cross sections profile of a Pt-core/Au-shell nanoparticle is comparable to the UV–Vis absorption spectrum of bimetallic nanoparticles. This suggests that the systems obtained correspond to core/shell type nanostructures. In this case the scattering cross section is the best agreement theoretical calculation in comparison with experimental results. Thus, the synthesis process mentioned above can be applied to obtain bimetallic nanostructures according to the parameters used, mainly the combination time of the metal precursors.

**Acknowledgments** The author O. Rocha-Rocha acknowledges support from CONACYT scholarships. The author M. Cortez-Valadez acknowledges support Project A1-S-46242 of the CONACYT Basic Science.

**Conflict of interest** The authors declare that there are no conflicts of interest related to this article.

## References

1. J.K. Majhi, and P.K. Kuiri, *J. Nanoparticle Res.* 22, 1 (2020).
2. L. Wang, Z. Wang, L. Li, J. Zhang, J. Liu, J. Hu, X. Wu, Z. Weng, X. Chu, J. Li, and Z. Qiao, *RSC Adv.* 10, 2661 (2020).
3. A. Higareda, S. Kumar-Krishnan, A.F. García-Ruiz, J. Maya-Cornejo, J.L. Lopez-Miranda, D. Bahena, G. Rosas, R. Pérez, and R. Esparza, *Nanomaterials* 9, 1644 (2019).
4. T. Bian, H. Zhang, Y. Jiang, C. Jin, J. Wu, H. Yang, and D. Yang, *Nano Lett.* 15, 7808 (2015).
5. A.L. Aden, and M. Kerker, *J. Appl. Phys.* 22, 1242 (1951).
6. Y. Nomura, and K. Takaku, *J. Phys. Soc. Japan* 10, 700 (1955).
7. J.R. Wait, *Appl. Sci. Res. Sect. B* 10, 441 (1962).
8. R.W. Fenn, and H. Oser, *Appl. Opt.* 4, 1504 (1965).
9. W.F. Espenscheid, E. Matijević, and M. Kerker, *J. Phys. Chem.* 68, 2831 (1964).
10. G.W. Kattawar and D.A. Hood, Appl. Opt. (1976)
11. S. Mandal, A.B. Mandale, and M. Sastry, *J. Mater. Chem.* 14, 2868 (2004).
12. A.S. Lapp, Z. Duan, N. Marcella, L. Luo, A. Genc, J. Ringnalda, A.I. Frenkel, G. Henkelman, and R.M. Crooks, *J. Am. Chem. Soc.* 140, 6249 (2018).
13. J. Yang, J. Yang Lee, and H.P. Too, *Plasmonics* 1, 67 (2006).
14. W. Zhang, L. Li, Y. Du, X. Wang, and P. Yang, *Catal. Letts.* 127, 429 (2009).

15. O. Rocha-Rocha, M. Cortez-Valadez, G. Calderón-Ayala, C.E. Martínez-Nuñez, M. Pedroza-Montero, and M. Flores-Acosta, *Phys. Lett. Sect. A Gen. At. Solid State Phys.* 383, 125985 (2019).
16. C.F. Bohren, and D.R. Huffman, *Absorption and scattering of light by small particles* (Hoboken: Wiley, 1983).
17. J.D. Jackson, *Classical Electrodynamics* (Hoboken: Wiley, 1999).
18. R. Rodríguez-Mijangos, and R. García-Llamas, *Rev. Mex. Física E* 62, 51 (2016).
19. E.D. Palik, *Handbook of Optical Constants of Solids* (Cambridge: Academic Press, 1998).
20. K.S. Lee, and M.A. El-Sayed, *J. Phys. Chem. B* 110, 19220 (2006).
21. J. Luo, L. Wang, D. Mott, P.N. Njoki, Y. Lin, T. He, Z. Xu, B.N. Wanjana, I.I.S. Lim, and C.J. Zhong, *Adv. Mater.* 20, 4342 (2008).
22. K.L. Kelly, E. Coronado, L.L. Zhao, and G.C. Schatz, *J. Phys. Chem. B* 107, 668 (2003).
23. I.O. Sosa, C. Noguez, and R.G. Barrera, *J. Phys. Chem. B* 107, 6269 (2003).
24. U. Kreibig, and M. Vollmer, *Optical properties of metal clusters* (Berlin: Springer, 2013).
25. H. Hövel, S. Fritz, A. Hilger, U. Kreibig, and M. Vollmer, *Phys. Rev. B* 48, 18178 (1993).